Composite columns built in cross-shaped section steel

Autor(en): **Ono, Tetsuro / Kimura, Mamoru / Kawabe, Haruhiko**

Objekttyp: **Article**

Zeitschrift: **IABSE reports = Rapports AIPC = IVBH Berichte**

Band (Jahr): **60 (1990)**

PDF erstellt am: **23.07.2024**

Persistenter Link: https://doi.org/10.5169/seals-46464

Composite Columns Built in Cross-Shaped Section Steel

Poteaux mixtes à armature d'acier de section cruciforme

Verbundstützen mit eingebautem Kreuzförmigen Profilstahl

Tetsuro ONO
Professor
Nagoya Inst. of Tech.
Nagoya, Japan

Mamoru KIMURA
Chief Res. Eng.
Takenaka Techn. Res. Lab.
Tokyo, Japan

Haruhiko KAWABE
Structural Eng.
Takenaka Corp.
Osaka, Japan

Hideki IDOTA
Res. Associate
Nagoya Inst. of Tech.
Nagoya, Japan

SUMMARY
In order to simplify the connection, to improve the filling capacity of concrete, and to reduce the weight of steel, the authors propose the use of a composite column built-in cross-shaped section steel without a flange is built. In this paper, the resistance and restoring force characteristics of this composite column are explained with the repeated shear bending test under high axial loading.

RÉSUMÉ
Afin de simplifier la connexion, d'améliorer la capacité de remplissage du béton et de réduire le poids de l'armature d'acier, les auteurs proposent l'utilisation d'un poteau mixte dans lequel est incorporée une armature d'acier de section curciforme sans bride. Dans le présent document, la résistance et la force de rappel qui constituent les caractéristiques de ce poteau mixte sont expliquées au moyen de l'essai répété à la flexion et au cisaillement sous un effort axial élevé.

ZUSAMMENFASSUNG
Um die Verbindung zu vereinfachen, die Füllungskapazität zu verbessern und das Stahlgewicht zu verringern, empfehlen die Autoren die Verwendung von Verbundstützen, in die ein kreuzförmiger Profilstahl ohne Flansch eingebaut ist. In diesem Bericht werden die Widerstands- und Rückstellkräfte dieser Verbundstütze unter wiederholtem Druckschub-Belastungstest bei hoher Schubbelastung dargestellt.

1. INTRODUCTION

The reinforcement of the beam-column connection of SRC structure will become complicated, whichever method is used, the column penetration method or the beam penetration method. The fact that the connections in the SRC structure are comlicated is exercising adverse effects on the construction operation, construction period, cost or structural design of the SRC structure.
Therefore, the authors propose SRC member, which incorporate flange-less cruciform section steel in order to simplify the beam-column connection, to imporove the fillability of concrete and to reduce the steel weight. These SRC columns expect to be benefited by the reinforcing effect against shearing of cruciform section steel. The present study is aimed at putting these SRC column to a flexural shearing test under high axial force and to find out its dynamical characteristics.

2. TEST PLAN AND SPECIMEN SHAPES

Specimen shapes are shown in Fig.1. The specimens are meant for the lower-story column of high and medium-high buildings and are scaled down to about 1/5 of actual buildings. Their shear span ratio (h/D) is 2.44. The outline of the specimens is shown in Table 1. Test parameters are the shape and thickness of steel, hoop ratio and sectional area of main reinforcement.
For specimens of Types A, B, and C, shapes and plate thickness of the steel have been changed in order to observe the shearing reinforcement effect of the steel. For Type A, hoop ratio Pw is set at a rather larger value of 0.72 (%), in order to find out the constraint effect of the hoop. For specimens of Type D, sectional areas of steels are the same, but the length of cruciform steel is changed. For Type E-1, the sectional area of main reinforcement is set at double that of the basic cross section. For Type F-1, the surface of the steel is coated with 2-mm-thick wax in order to remove the bond between steel and concrete. The test set-up are shown in Fig.2. The load has been applied gradually with the anti-symmetric bending moment in repetition of positive and negative alternation. The angle of relative displacement has been calculated from the relative displacement, corresponding to member shearing deformation measured, and displacement in the material length direction. For strain, axial-direction strain and shearing strain of steel members and axiald-direction strain of main reinforcement and hoop are measured by monoaxial and triaxial strain gages. Checking condition is measured by visual inspection.

3. TEST RESULTS

3.1 Test Process and Failure Condition

At all specimens excepting Types D2 and D3, oblique cracking and shear bond cracking were observed accompanying diagonal tension at an angle of relative displacement of R =0.002 rad. All specimens reached the maximum yielding strength at R =0.005 to 0.01 rad, and then shear bond cracking rapidly progrssed at all specimens except for Type D3. All specimens excepting Type D3 came to show distinct peeling-off of concrete at R =0.01 to 0.015 rad. The cracking condition of all specimens at R =0.02 rad is shown in Fig.3. The collaps mode of all specimens excluding Type D3 was shear bond failure. The collapse mode of Type D3 was shear compression failure. Further, steel buckling was observed in Type D3, and yield strength thereafter suddenly dropped.

3.2 Hysteresis Characteristics and Ultimate Strength

Bending strength curves (M-N interaction) of specimens Types A2, B2 and D

according to the general additive strength theory are shown in Fig.4. All specimens have developed shearing bond failure (except Type D3 which has shown shearing compression failure), and test values lie at the inside of the curve. The Q-δ curves obtained by the present test are shown in Fig.5. In these Figures, the ordinate represents shearing force Q, and the abscissa represents the relative displacement δ of the capital and base of the column and the angle of relative displacement R. The dot-dash line shows the strength drop slope due to the P-δ effect of axial force. Hysteresis curves of Types B2 and D1, which have basic cross sections, indicate spindle shapes which show the significant quantities of stabilized energy absorption. Further, in Type B3, which contains thick steel, a strength drop has not been observed, even if the angle of relative displacement has dropped to R =0.03 rad. On the other hand, Type C2 which has the low height of the cruciform section steel and Type D3 having a rectangular section steel have shown brittle failure. Type D3 has shown sudden strength drop after the ultimate strength, and showed a significant drop from the envelope curve of the repetitive loop at an angle of relative displacement of R =0.01 rad. In the Type D series with the effective width b' of concrete as a parameter, the ultimate strength rises depending upon the magnitude of the effective width, but tougness tends to drop. The reason for the rise in the ultimate strength of Type E1 is the addition of the strength of truss mechanism. Further, the hysteresis curves of Types D2 and E1 tend to converge on the hysteresis curve of Type D1. In these specimens, the ultimate strength of arch mechanism and truss mechanism at the reinforced concrete portion runs counter to the increase in deformation capacity.

4. STRENGTH SHEARING CONDITION

Ultimate strength obtained by the test is dissolved into the following sectional-area elements to calculate the respective burden strength values (refer to Fig.6).

(A) Cruciform section steel
(B) Truss mechanism portion consisting of reinforcement, loop and concrete bundles having a width of $_{r}b$
(C) Arch mechanism portion consisting of only plain concrete

Table 2 shows the shared axial force of various elements at the time 1) when only axial force acts which has been obtained from axial strain of steel and reinforcement and 2) when the maximum stength acts. Shared axial force of steel is about 50% of yield axial force.
Fig.7 shows the shared bending moments of various elements. Fig.8 shows shared shear force of various elements.

5. DISCUSSION

5.1 Sharing of Axial Force

The axial force of the SRC column built-in cruciform section steel is shared by steel and plain concrete. Since the shared bending moment of steel at the time of the maximum strength has reached full plastic moment sMp, it can be assumed that the shared axial force of steel is borne only by the horizontal cross section element of the crusiform section steel. Therefore, the axial force of the SRC member can be expressed by the following formula:

$$N = (A_s/2)\cdot {}_s\sigma_y + \alpha\cdot F_c\cdot b\cdot D$$

where A_s: Sectional area of steel, $_s\sigma_y$: yield stress of steel

5.2 Sharing of Bending

At the time of R =0.002 rad, the bending moments of all specimens are still

shared according to rigidity. Then, as the value of the angle of relative displacement increases, the share of the steel part has become larger. The share of the steel plat shows the value of the full plastic moment at the time of maximum strength, and later is maintained at a constant value. From Fig.7, after the maximum strength is reached, the collapse of concrete progresses, and shares of the truss mechanism part and arch mechanism part have dropped. This drop in sharing at the truss mechanism part ($_{rc}M$) and arch mechanism part ($_{co}M$) is considered directly affecting the drop in toughness.

5.3 Sharing of Shear Force

Shared shear force values of various elements correspond to the respective shared bending moments, until the maximum strength is reached. However, the shared shear force values elements, after the maximum strength is reacfhed, show an increase in the shared value at the steel part and a decrease in the shared value at the arch mechanism part. This suggests that there is a sort of stress transferring between the steel element and other elements.

5.4 Reinforcing Effect against Shearing of Cruciform Section Steel

Fig.9 shows an example of the distribution of shearing strain on steel member. The distribution of shearing strain becomes a parabola distribution in the case of cruciform section steel which has no valve. Further, Type B1, which has a valve, develops an overall rise in shearing strain compared with Type B2 without value. This may be attributable to the increase in the geometrical moment of area and the stress transferring effect to the steel part. Now the shear strain distributions of Types C2 and D are considered which use the width of the horizonatal element of steel as a parametter. The shearing strain level of Type C2 shows a smaller value compared with that of Type B2, but Type D has reached virtually the same strain level as Type B2. Since Type C2 can be assumed to be on SRC member having axial steel, the shared shear force of steel is little, and the hystresis characteristics has also deteriorated. Fig.10 shows 1) shear force $_{s}Q_{m}$ calculated from the shared bending moment of the material end of steel and 2) shear force $_{s}Q$ calculated from the triaxial gage at the center part of the steel member. In the elastic state, the trend of $_{s}Q = {}_{s}Q_{m}$ is shown, and after the maximum strength, the trend of $_{s}Q > {}_{s}Q_{m}$ becomes distinct. These facts may be contributing to the stability of the hysteresis characteristic after the maximum strength.

6. CONCLUSION

1) The specimen of the SRC column with built-in cruciform section steel shows, even under high axial force, a stabilized spindle-shape hysteresis curve, by not being very much affected by the thickness of steel plate, if only the height of the steel is sufficient.
2) It is considered that in the specimen of the SRC column with built-in cruciform section steel, the cruciform section steel seems to have a sufficient reinforcing effect against shearing.

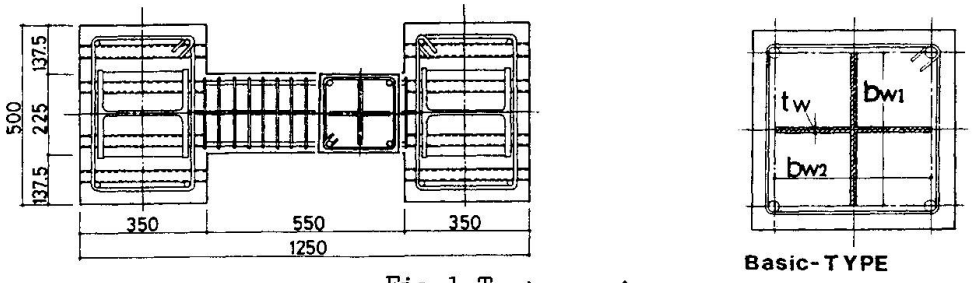

Fig.1 Test specimen

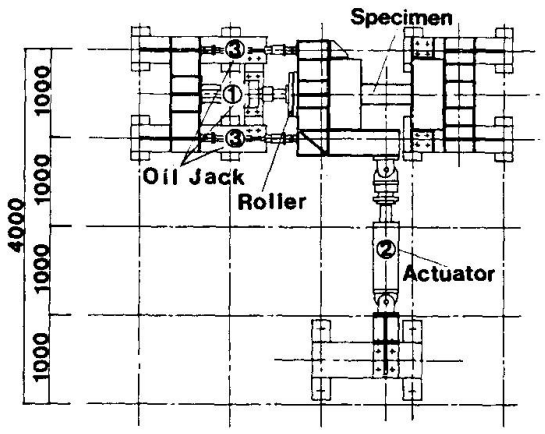

Fig.2 Test set-up

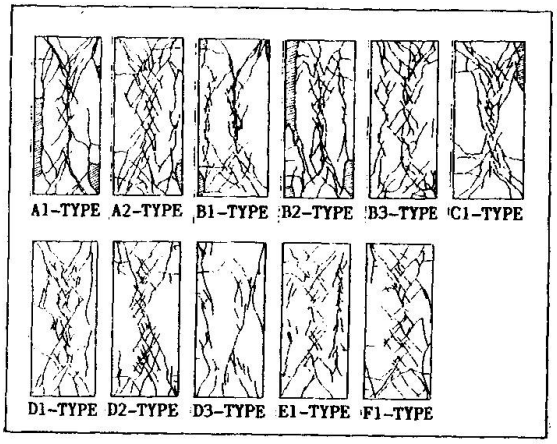

Fig.3 Crack pattern

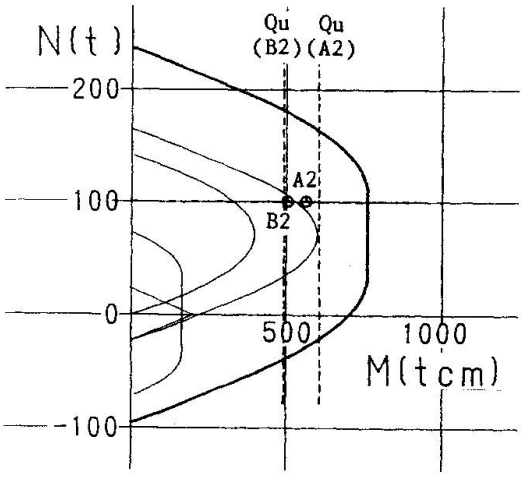

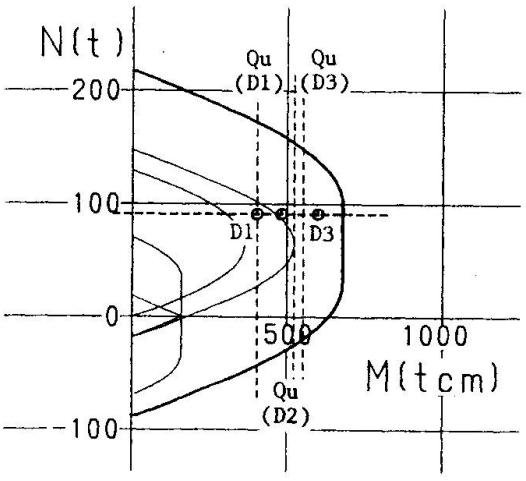

Fig.4 M-N interaction

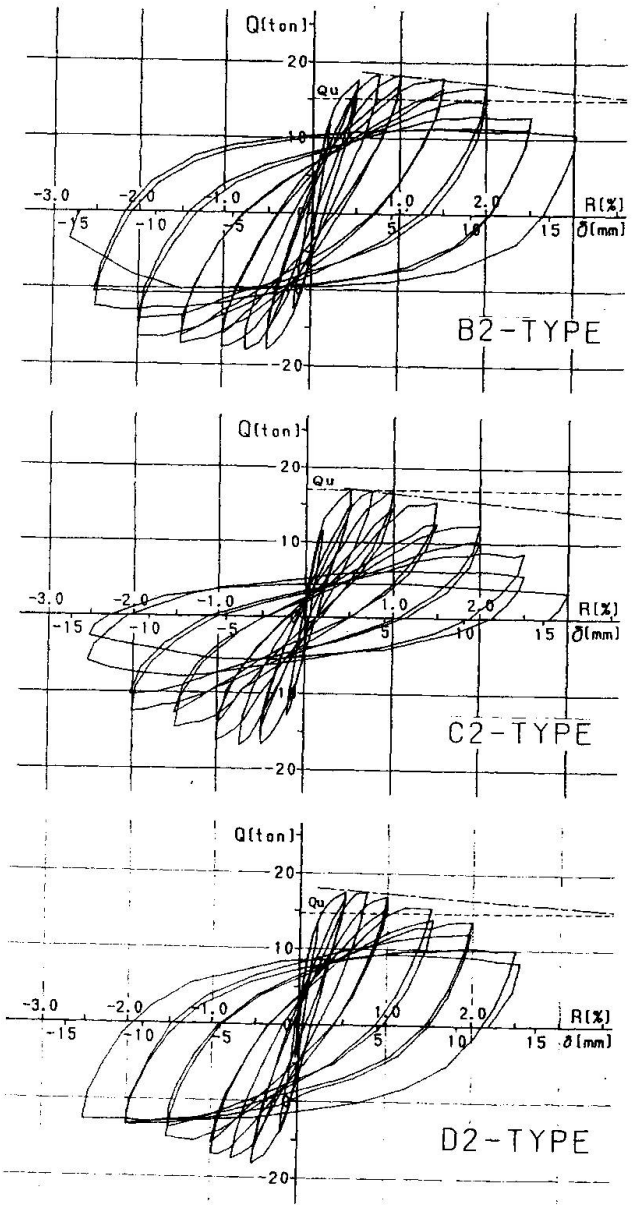

Fig.5 Q-δ curves

TEST No.	CRUCIFORM SECTION STEEL $b_{w1}\times b_{w2}$	t_w	σ_y(t/cm^2)	HOOP SECTION	p_w(%)	MAIN REI.	CONCRETE Fc(kg/cm^2)
A 1	175×175	3.2	3.24	6φ-@35	0.72	4-D13	280
A 2	175×175	6.0	3.49	6φ-@35	0.72	4-D13	280
B 1	175×175	6.0	3.49	4φ-@40	0.28	4-D13	280
B 2	175×175	6.0	3.49	4φ-@40	0.28	4-D13	280
B 3	175×175	9.0	2.77	4φ-@40	0.28	4-D13	280
C 1	175×175	6.0	3.49	4φ-@40	0.28	4-D13	280
C 2	87.5×87.5	12.0	2.80	4φ-@40	0.28	4-D13	255
D 1	175×175	6.0	3.38	4φ-@40	0.28	4-D13	255
D 2	87.5×175	[6.0 [12.0	[3.38 [2.80	4φ-@40	0.28	4-D13	255
D 3	175 -	12.0	2.77	4φ-@40	0.28	8-D13	255
E 1	175×175	6.0	3.38	4φ-@40	0.28	4-D13	255
F 1	175×175	6.0	3.38	4φ-@40	0.28	4-D13	255

Table 1 Dimensions of test specimen

TEST No.	SHARE OF AXIAL FORCE Q=0 sN(t),	rcN(t),	coN(t)	Q=Qmax sN(t),	rcN(t),	coN(t)
A 1	21.2	4.4	74.4	18.5	3.9	77.6
A 2	33.2	2.1	64.7	41.5	1.1	57.4
B 1	33.6	4.1	62.3	41.5	0.6	57.9
B 2	25.7	8.9	65.4	28.6	11.6	59.8
B 3	42.6	7.7	49.7	53.1	7.3	39.6
C 1	28.4	7.7	63.9	41.5	6.7	51.8
C 2	23.9	7.4	68.7	19.1	7.1	73.8
D 1	23.7	5.7	70.6	27.4	4.8	67.9
D 2	23.6	5.6	70.8	29.2	4.6	66.2
D 3	24.1	6.3	69.6	17.7	6.2	76.1
E 1	22.5	10.6	66.9	30.5	9.6	40.1
F 1	23.8	5.7	70.5	31.9	5.7	62.4

Table 2 Shared axial force of element

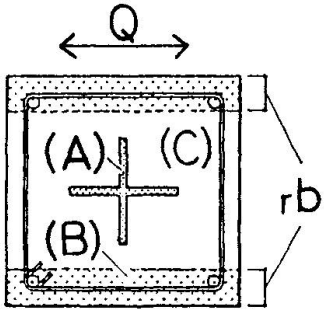

Fig.6 Calculate elements

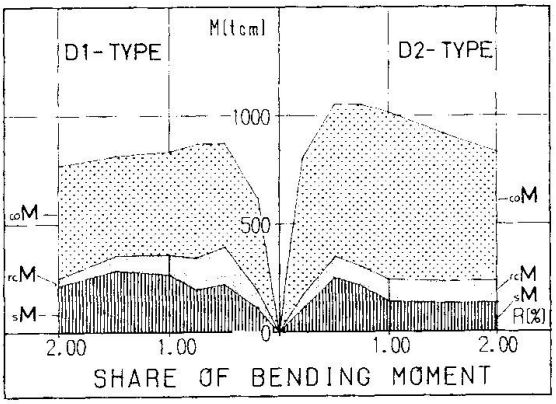

Fig.7 Share of bending moment

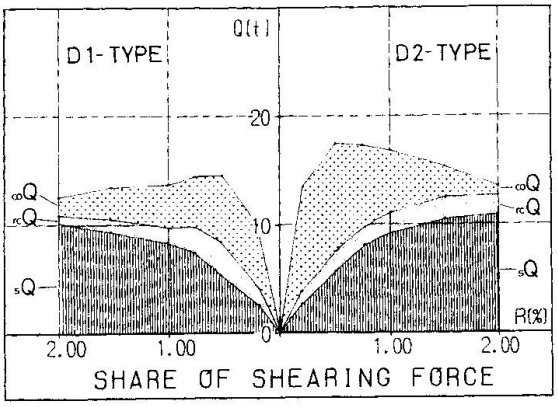

Fig.8 Share of shear force

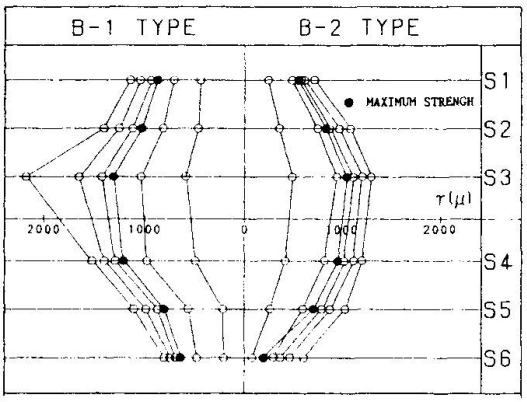

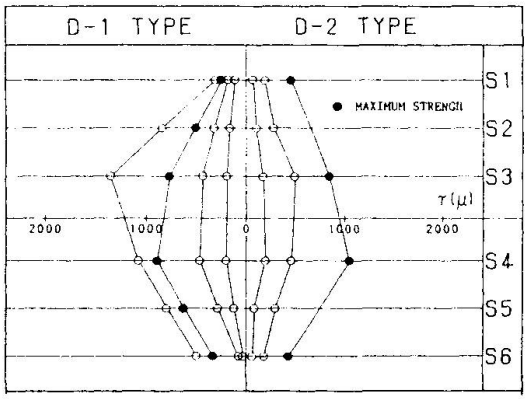

Fig.9 Distribution of shearing strain of steel member

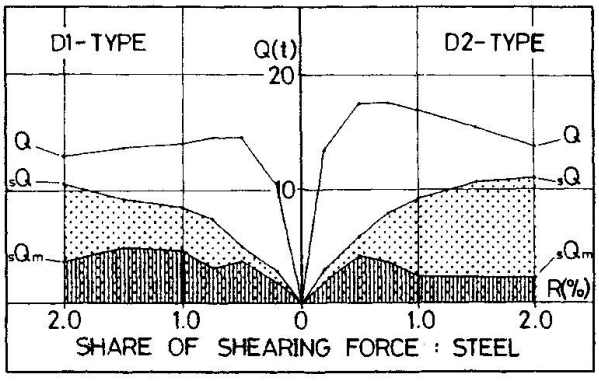

Fig.10 Share of shear force on steel member